

# RETINAL VESSEL SKELETONIZATION USING SCALE-SPACE THEORY

Pattheera Panitsuk<sup>(1)</sup>, Prach Viboontapachart<sup>(1)</sup>, Touchapong Prukthichaipat<sup>(1)</sup>, Bunyarit Uyyanonvara<sup>(1)</sup>,  
Chanjira Sinthanayothin<sup>(2)</sup>

(1) Sirindhorn International Institute of Technology, Pathumthani, Thailand 12120

(2) NECTEC, National Science and Technology Development Agency

Pathumthani Thailand 12121 E-mail: chanjira.sinthanayothin@nstda.or.th

## ABSTRACT

In this paper we introduce the alternative method for blood vessel extraction based on scale space theory. The original image is converted into gray level image and it is then blurred with Gaussian Blur using many kernel sizes. Each kernel produces an image at that particular scale. Edge detection is applied to each result using Laplace algorithm. Noises are then removed using adaptive median filter. Images are converted to binary images and the isolated islands are removed using region growing technique. Candidate vessels from all scales are combined for the final result. The algorithm was tested on 100 images and the results are compared with ophthalmologists' hand-drawn ground truth. The performance is very encouraging and it can detect the blood vessel with a high specificity of 0.9698.

**Index Terms**— vessel skeletonization, noise reduction, isolated island removal, scale space, retinal vessel extraction.

## 1. INTRODUCTION

Retinal blood vessel analysis has become more common in the medical diagnosis system because of many reasons. One important reason of them is that the retinal blood vessel can be used to diagnose many diseases.

There are many works have been proposed to extract skeleton of retinal blood vessels. Martinex-Perez et al [1] was using a semi-automatic method to measure and quantify the geometrical and topological properties of retinal blood vessel from fundus retinal images with is based on multi-scale analysis to detect the vessel. However the method is very complex and requires a lot of steps in order to obtain the final result. There were also many literatures proposing the vessel extraction using matched filter such as Canny. Chanwimaluang and Fan [2] and Gao et al [3] introduced efficient methods for automatic detection and extraction of blood vessels. Canny [4] experimented with an algorithm of matched filters for vessel detection and Chaudhuri [5] used a Gaussian vessel cross-sectional profile and assumed Gaussian imaging noise for vessel detection using matched

filters. However, main disadvantage of the method is its high computational cost. They are usually implemented as a convolution of an image with a set of oriented segments, which is especially expensive when computed at multiple scales. A method of registration of retinal images based on feature detection was reported by Byrne et al [6]. Line finding algorithms along with a probabilistic relaxation scheme has been proposed to extract and describe the blood vessel pattern in retinal images by Akita [7-9]. These segments were later connected to a vessel network and labeled as arteries or veins according to their chromatic information. Toliás and Panas [10] developed a fuzzy C-means (FCM) clustering algorithm that uses linguistic descriptions like “vessel” and “nonvessel” to track fundus vessels in retinal angiogram images. Though, the weak point of the fuzzy C-means (FCM) is that the fuzzy C-means (FCM) is very sensitive to noises so the sensitivity of the output may be low compared to the others. Gang et al [11] showed the Gaussian curve is suitable for modeling the intensity profile of the cross section of retinal vessels in color fundus images. Neural network application is proposed by Sinthanayothin et al [12]. It employed intensity edge detection and principal component analysis of input images as inputs to multilayer perceptron neural networks to identify blood vessels. Nekovei and Sun [13] detected blood vessels in XRA images using a back-propagation network. Leandro et al [14] used a continuous wavelet transform combined with morphological operators to segment blood vessels within the retina. Staal [15] presented a method to detect vessels by proposing a more natural representation for elongated structures, such as vessels. Parvin et al [16], Huang and Stockman [17], and Aylward et al [18] described similar algorithms that used generalized cylinders to extract tubular structures in 2D intensity images.

Many techniques mentioned above required priori information about the structure and approximate size of the vessel. In this paper, we propose to extract skeleton of vessel based on scale space theory. Scale space theory was first proposed by Witkin[19] and Koenderink [20] to obtain a multi-scale representation of a measured signal by embedding it into a scale-parameter family of blurred signals. The scale-space analysis employs blurring the input

image so that the objects are smoothed and eventually turn into the so-called light blobs.

## 2. METHODOLOGY

Image is transformed to grey scale before it is blurred with 5 different Gaussian kernel of size 3x3, 5x5, 7x7, 9x9, and 11x11 to generate 5 different scales of the original image. A Laplace edge detection algorithm with kernel size 7 was applied to the images of all scales. Adaptive Median Filter with the kernel size that can automatically, adaptively be adjusted from 3x3 to 7x7 was applied for noise reduction. The images are then binarized. The bigger noise are removed with isolated island removal technique. All 5 final results from all scales are combined to generate a final output. The overall process is illustrated in Fig. 1. Each step in the process is experimentally optimized for this set of images and the details of each step are explained in the following sections.

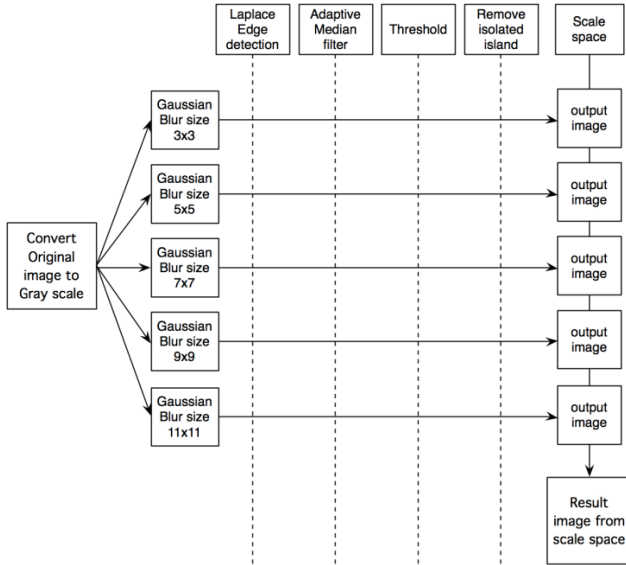


Figure 1: Process sequence of retinal vessel extraction

### 2.1 Gaussian blur

Five different sizes of Gaussian kernel, 3x3, 5x5, 7x7, 9x9 and 11x11 are used to represent each image in different scale. The Gaussian kernel is represented by Eq. (1) and Eq. (2).

$$G(x, y) = \frac{1}{2\pi\sigma^2} e^{-\frac{x^2+y^2}{2\sigma^2}} \quad \dots (1)$$

$$\sigma = \left(\frac{n}{2} - 1\right) \times 0.3 + 0.8 \quad \dots (2)$$

### 2.2 Laplace edge detection

All image from 5 scaled received from a previous step are processed with edge detection. In this step, Laplace edge detection, as in Eq. (3), is selected to detect the blood vessel and examples of the results are shown in Fig 2.

$$dst(x, y) = \frac{d^2 src}{dx^2} + \frac{d^2 src}{dy^2} \quad \dots (3)$$

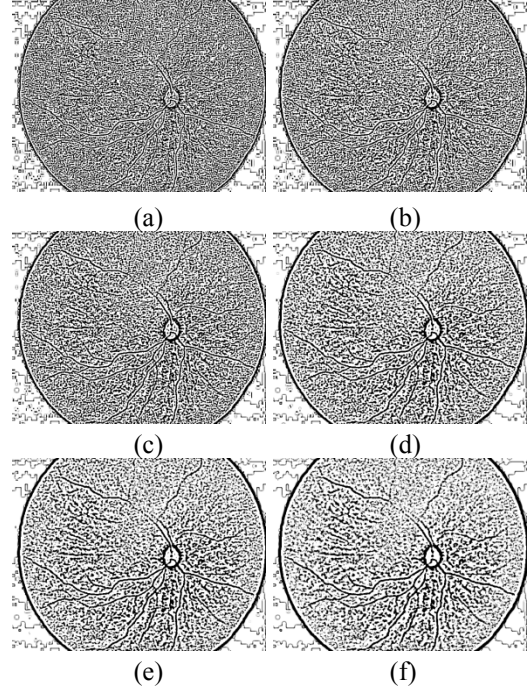


Figure 2: The sample images that have been applied the edge detection using Laplace algorithm. The image (a) shows the image that does not apply any smoothing algorithm. (b),(c),(d),(e) and (f) represent the sample image that apply Gaussian blur in the gray scale image with the kernel size of 3x3, 5x5, 7x7, 9x9 and 11x11 respectively.

### 2.3 Adaptive Median filter

Speckle noise can be removed from the previous result using adaptive median filter. The adaptive median filter will first find the median of the value obtain from the intensity in kernel, and then compare it with the mean value of the kernel. If different of the median value and the mean value is not less than standard deviation, then the kernel size increases. However, if the value that satisfied the condition does not exist, then the smallest size of kernel that has different between mean value and median value is selected. Hence, the kernel size is adaptively adjusted between 3 and 7.

### 2.4 Isolated island removal

Images are binarized prior to this step. In this step, we count the number of connected pixels. If the size of the island is smaller than a certain limit then that island will be removed. We experimentally tried 3 different values, 300, 400 and 500 as an example shown in Fig 3. We found that 500 is the best limit for this set of images.

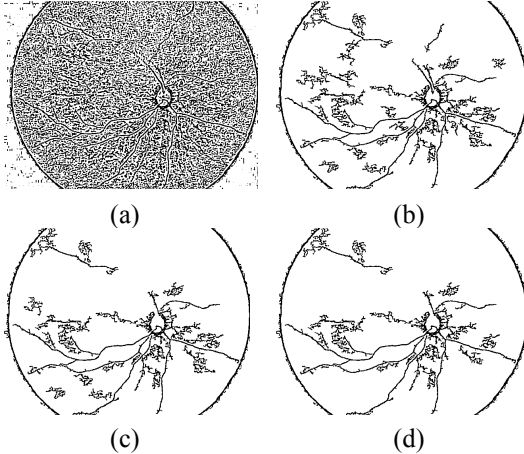


**Figure 3:** Result of island removal (a) results from previous step. (b), (c) and (d) are results from isolated island removal with the limit of 300, 400, and 500 respectively.

### 2.5 Scales combination

All resulting images from all scales are combined in this step. The technique applied to the finest scale produces lots of unwanted noise while the application of the technique to the coarser scale also result in missing vessels but significantly less noise. For the scale combination, we aligned the images one on top of another from the finest scale (3x3) to the coarsest scale (7x7). Any pixels that appear in 3 or more consecutive scales will be marked as vessels pixels. This step mimics blob linking in the original scale space representation. The example results at each scale are displayed in Fig. 4 and the example from overall process is also illustrated in Fig 5

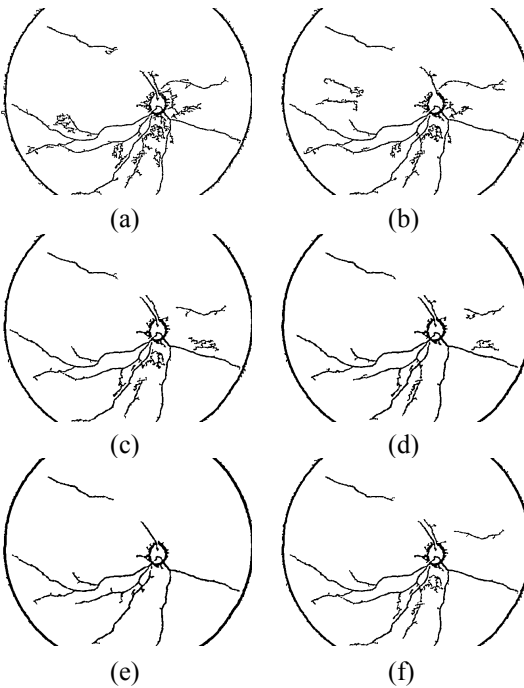


**Figure 4:** Example of image at different scales. (a),(b),(c), (d) and (e) represent images at scale 3x3, 5x5, 7x7, 9x9 and 11x11 respectively. (f) result after of all 5 scales combined.

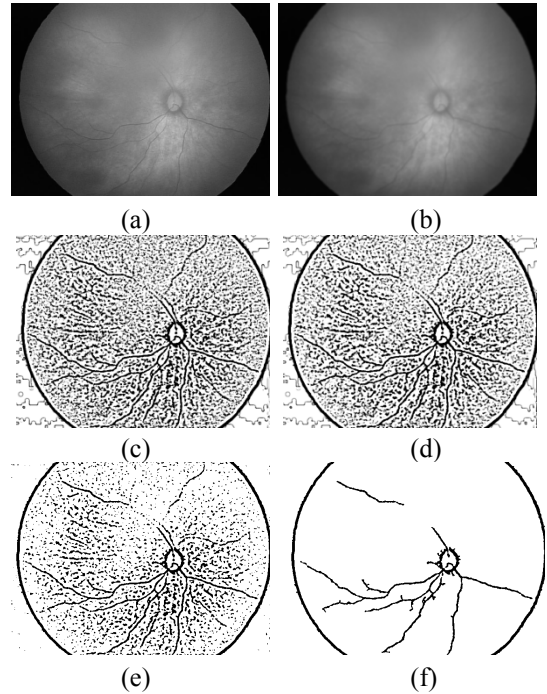


**Figure 5:** Examples of resulting images from each processing steps. (a) The gray scale image (b) Gaussian blur with kernel size 11x11 (c) Edge detection using Laplace algorithm (d) Adaptive median filter (e) Binary image (f) Isolated island removal and final result.

## 3. RESULT

A set of 100 test images are used in to test the algorithm. These 100 test images are grouped together into four testing groups based on their similar characteristics and clinicians suggestions, namely group A, B, C, and D. Group A contains images with fairly clear vessels while vessels in images in group B are difficult to distinguish. In group C, vessels of images are very convoluted while the vessels in images in group D are less convoluted.

The prediction results will be evaluated against clinician's hand drawn ground truths. Sensitivity and specificity are selected to measure the accuracy of the algorithms. This pixel-based evaluation considers four values, true positive (TP), a number of pixels correctly detected, false positive (FP), a number of non-vessel pixels which are detected wrongly as vessel, false negative (FN), a number of vessel pixels that were not detected and true negative (TN), a number of non- vessel pixels which were correctly identified as non- vessel. From these quantities, the sensitivity, specificity can be computed with Eq. (4) and (5).

$$\text{Sensitivity} = \frac{TP}{TP+FN} \quad \dots (4)$$

$$\text{Specificity} = \frac{TN}{TN+FP} \quad \dots (5)$$

Example of original images, their ground-truth and corresponding detection results are displayed in Fig. 6. Table 1 shows the quantitative results from the randomly selected 25 images. Fig. 7 and Fig. 8 are graphs of sensitivity and specificity of all test images and relationship between the two values respectively.

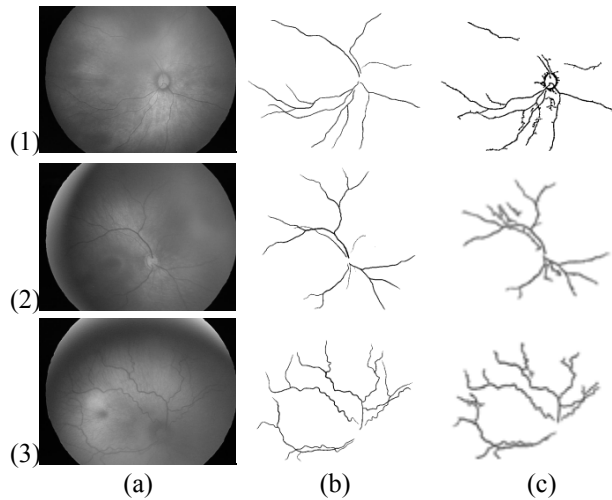


**Figure 6:** Example of original images, ground truths, and the resulting images.

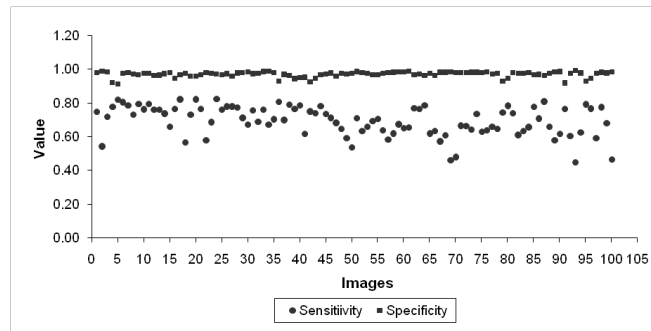


**Figure 7:** Sensitivity and specificity of all test images

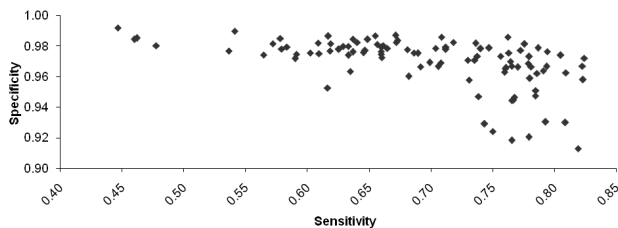


**Figure 8:** The relation between specificity and sensitivity

no	Set A		Set B		Set C		Set D	
	Sn	Sp	Sn	Sp	Sn	Sp	Sn	Sp
1	0.75	0.97	0.78	0.97	0.71	0.99	0.64	0.98
2	0.54	0.99	0.78	0.96	0.63	0.98	0.66	0.97
3	0.72	0.98	0.77	0.98	0.66	0.97	0.65	0.98
4	0.78	0.92	0.71	0.98	0.69	0.97	0.74	0.93
5	0.82	0.91	0.67	0.98	0.71	0.97	0.78	0.95
6	0.81	0.97	0.76	0.97	0.64	0.98	0.74	0.93
7	0.79	0.98	0.69	0.98	0.58	0.98	0.61	0.98
8	0.73	0.97	0.76	0.99	0.62	0.98	0.63	0.97
9	0.79	0.97	0.67	0.99	0.67	0.98	0.66	0.98
10	0.76	0.98	0.7	0.98	0.65	0.98	0.79	0.97
11	0.79	0.98	0.81	0.93	0.65	0.99	0.71	0.97
12	0.76	0.96	0.7	0.97	0.77	0.97	0.81	0.97
13	0.76	0.97	0.79	0.96	0.76	0.97	0.66	0.98
14	0.74	0.97	0.77	0.94	0.79	0.96	0.58	0.99
15	0.66	0.98	0.78	0.95	0.62	0.98	0.62	0.99
16	0.77	0.94	0.62	0.95	0.63	0.96	0.77	0.92
17	0.82	0.97	0.75	0.92	0.57	0.98	0.6	0.98
18	0.56	0.97	0.74	0.92	0.61	0.98	0.45	0.99
19	0.73	0.96	0.74	0.95	0.46	0.98	0.63	0.98
20	0.82	0.96	0.74	0.97	0.48	0.98	0.79	0.93
21	0.77	0.97	0.71	0.98	0.66	0.98	0.77	0.95
22	0.58	0.98	0.68	0.96	0.66	0.98	0.59	0.97
23	0.69	0.98	0.65	0.98	0.64	0.98	0.78	0.98
24	0.82	0.97	0.59	0.97	0.74	0.98	0.68	0.98
25	0.76	0.97	0.54	0.97	0.63	0.98	0.46	0.99
Mean	0.74	0.97	0.72	0.96	0.65	0.98	0.67	0.97

**Table 1:** Quantitative detection results. (Sn: Sensitivity, Sp: Specificity)

#### 4. DISCUSSION AND CONCLUSION

From the result, even though the specificity is very high, the sensitivity is relatively low. Also the specificity of all data set are very close but the sensitivity are varied and depending on the quality of the data set. We also found that the efficiency of the algorithm depends very much on the edge detection results. The output from edge detection step usually does not contain all of blood vessel especially the end-point. This can be improved by choosing a more appropriate edge detection algorithm which is not the main point of this paper.

This paper presents an alternative method for blood vessel extraction based on scale space algorithm. The experiment results demonstrated that the propose method can detect blood vessel efficiently with specificity as high as 0.97. The algorithm will be a useful part for the further use in medical analysis.

## 5. ACKNOWLEDGEMENT

The project is financially supported by Young Scientist Technologist Program, NSTDA (YSTP: SP-52-NT-14).

## 6. REFERENCES

- [1] Martinez-Perez ME, Hughes AD, Stanton AV, Thom SA, Chapman N, Bharath AA, et al. Retinal vascular tree morphology: a semi-automatic quantification. *IEEE Trans Biomed Eng* 2002; 49: 912-7.
- [2] Chanwimaluang T, Fan G. An efficient algorithm for extraction of anatomical structures in retinal images. *Image Processing, In Proceedings. 2003 International Conference. Barcelona, Spain; 14-17 Sept, 2003.*
- [3] Gao XW, Bharath A, Stanton A, Hughes A, Chapman N, Thom S. Quantification and characterisation of arteries in retinal images. *Comput Methods Programs Biomed* 2000; 63: 133-46.
- [4] Canny J. A computational approach to edge detection. *IEEE Trans Pattern Anal Mach Intell* 1986; 8: 679-98.
- [5] Chaudhuri S, Chatterjee S, Katz N, Nelson M, Goldbaum M. Detection of blood vessels in retinal images using two dimensional matched filters. *IEEE Trans Med Imaging* 1989; 8: 263-9.
- [6] Byrne JPC, Ross PGB, Undrill PE, Philips RP. Feature based retinal image registration using transporter. *Appl Transputer* 1991; 3: 687-92.
- [7] Akita K, Kuga H. A computer method of understanding ocular fundus images. *Pattern Recognition* 1982; 15: 431-43.
- [8] Akita K, Kuga H. Digital processing of color ocular fundus images. in *MEDINFO' 80. Amsterdam, The Netherlands: North-Holland; 1980: 80-4.*
- [9] Akita K, Kuga H. Pattern recognition of blood vessel networks in ocular fundus images. in *IEEE Int. Workshop Phys. And Eng. In Med. Imaging, Mar 15-18, 1982: 436-41.*
- [10] Toliyas YA, Panas SM. A fuzzy vessel tracking algorithm for retinal images based on fuzzy clustering. *IEEE Trans Med Imaging* 1998; 17: 263-73.
- [11] Gang L, Chutatape O, Krishnan SM. Detection and measurement of retinal vessels in fundus image using amplitude modified second-order Gaussian filter. *IEEE Transaction on Viomedical Engineering, Vol. 49, No. 2, February 2002.*
- [12] Sinthanayothin C, Boyce JF, Cook HL, Williamson TH. Automated localisation of the optic disc, fovea, and retinal blood vessels from digital colour fundus images. *Br J Ophthalmol* 1999; 83: 902-10.
- [13] Nekovei R, Sun Y. Back-propagation network and its configuration for blood vessel detection in angiograms. *IEEE Trans. on Neural Nets* 1995; 6: 64-72.
- [14] Leandro JG, Cesar RM Jr, Jeline HF. Blood vessels segmentation in retina. Preliminary Assessment of the Mathematical Morphology and of the Wavelet Transform Technique SIBGRAPI 2001, XIV Brazilian Symposium on Computer Graphics and Image processing, 15-18 October 2001, Florianopolis, Brazil.
- [15] Staal JJ, Kalitzin SN, Abramoff MD, Berendschot T, van Ginneken B, Viergever MA. Classifying convex sets for vessel detection in retinal images. *Proceedings of the IEEE International Symposium on Biomedical Imaging. 2002: 269-72.*
- [16] Parvin BA, Penf C, Johnston W, Maestre FM. Tracking of tubular objects for scientific applications. in *Proc of the IEEE Conf on CVPR. 1994: 297-301.*
- [17] Huang Q, Stockman GC. Generalized tube model: recognizing 3d elongated objects from 2d intensity images. in *Proc of the IEEE Conf on CVPR. 1993: 104-9.*
- [18] Aylward S, Pizer S, Bullitt E, Eberl D. Intensity ridge and widths for tabular object segmentation and registration. in *Wksp on Math Methods in Biomed Image Analysis. 1996: 131-8.*
- [19] A. P. Witkin. "Scale-space filtering," In *Proc. 8th Int. Joint Conf. Art. Intell., Karlsruhe, West Germany. (1983) 1019-1022.*
- [20] J. J. Koenderink and A. J. van Doorn, "Generic neighbourhood operators," *IEEE Trans. Pattern Analysis and Machine Intell. (1992) 597-605.*